



Estimating regional fluxes of CO₂ and CH₄ using space-borne observations of XCH₄ : XCO₂

A. Fraser¹, P. I. Palmer¹, L. Feng¹, H. Bösch², R. Parker², E. J. Dlugokencky³, P. B. Krummel⁴, and R. L. Langenfelds⁴

¹School of GeoSciences, University of Edinburgh, Edinburgh, UK

²Department of Physics and Astronomy, University of Leicester, Leicester, UK

³US National Oceanic and Atmospheric Administration, Global Monitoring Division, Earth System Research Laboratory, Boulder, Colorado, USA

⁴Centre for Australian Weather and Climate Research, CSIRO Marine and Atmospheric Research, Aspendale, Victoria, Australia

Correspondence to: P. I. Palmer (paul.palmer@ed.ac.uk)

Received: 23 May 2014 – Published in Atmos. Chem. Phys. Discuss.: 17 June 2014

Revised: 28 October 2014 – Accepted: 29 October 2014 – Published: 8 December 2014

Abstract. We use the GEOS-Chem global 3-D atmospheric chemistry transport model to interpret XCH₄ : XCO₂ column ratios retrieved from the Japanese Greenhouse Gases Observing Satellite (GOSAT). The advantage of these data over CO₂ and CH₄ columns retrieved independently using a full physics optimal estimation algorithm is that they are less prone to scattering-related regional biases. We show that the model is able to reproduce observed global and regional spatial (mean bias = 0.7 %) and temporal variations (global $r^2 = 0.92$) of this ratio with a model bias < 2.5 %. We also show that these variations are driven by emissions of CO₂ and CH₄ that are typically 6 months out of phase, which may reduce the sensitivity of the ratio to changes in either gas. To simultaneously estimate fluxes of CO₂ and CH₄ we use a maximum likelihood estimation approach. We use two approaches to resolve independent flux estimates of these two gases using GOSAT observations of XCH₄ : XCO₂: (1) the a priori error covariance between CO₂ and CH₄ describing common source from biomass burning; and (2) also fitting independent surface atmospheric measurements of CH₄ and CO₂ mole fraction that provide additional constraints, improving the effectiveness of the observed GOSAT ratio to constrain flux estimates. We demonstrate the impact of these two approaches using numerical experiments. A posteriori flux estimates inferred using only the GOSAT ratios and taking advantage of the error covariance due to biomass burning are not consistent with the true fluxes in our experiments, as

the inversion system cannot judge which species' fluxes to adjust. This reflects the weak dependence of XCH₄ : XCO₂ on biomass burning. We find that adding the surface data effectively provides an “anchor” to the inversion that dramatically improves the ability of the GOSAT ratios to infer both CH₄ and CO₂ fluxes. We show that the regional flux estimates inferred from GOSAT XCH₄ : XCO₂ ratios together with the surface mole fraction data during 2010 are typically consistent with or better than the corresponding values inferred from fitting XCH₄ or the full-physics XCO₂ data products, as judged by a posteriori uncertainties. We show that the fluxes inferred from the ratio measurements perform best over regions where there is a large seasonal cycle such as Tropical South America, for which we report a small but significant annual source of CO₂ compared to a small annual sink inferred from the XCO₂ data. We argue that given that the ratio measurements are less compromised by systematic error than the full physics data products, the resulting a posteriori estimates and uncertainties provide a more faithful description of the truth. Based on our analysis we also argue that by using the ratios we may be reaching the current limits on the precision of these observed space-based data.

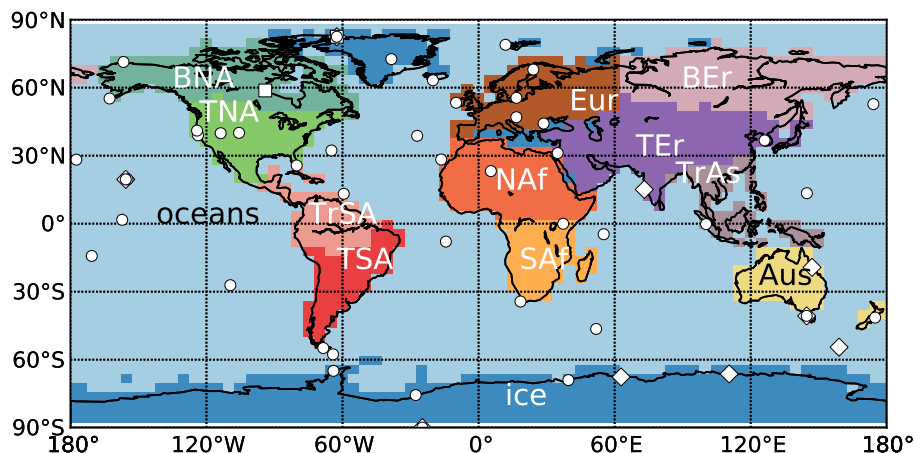


Figure 1. Distribution of the 13 geographical regions for which we estimate CO₂ and CH₄ fluxes, and the location of 57 co-operative flask sampling sites with data covering the study period, January–December 2010. The land regions, informed by previous work (Gurney et al., 2002), include Boreal North America (BNA), Temperate North America (TNA), Tropical South America (TrSA), Temperate South America (TSA), Northern Africa (NAf), Southern Africa (SAf), Boreal Eurasia (BEr), Temperate Eurasia (TEr), Tropical Asia (TrAs), Australasia (Aus), and Europe (Eur). The ground-based measurement sites run by NOAA ESRL, CSIRO GASLAB, and EC are denoted by white circles, white diamonds, and white squares, respectively.

1 Introduction

Space-borne atmospheric column measurements of CO₂ and CH₄ have the potential to improve our quantitative understanding of their surface fluxes and to underpin the development of testable climate policies. For these data to address these potential applications the column measurements have to meet strict precision requirements, reflecting small signals from surface fluxes (a few percent of the column amount) compared to the variations due to atmospheric transport. Any uncharacterized systematic error in these measurements compromises the ability of these data to infer surface fluxes. The CO₂ inverse problem is particularly sensitive to these systematic errors acting on length scales of 10³–10⁴ km, between the spatial scales of numerical models and those observed by the sparse network of well-characterized upward-looking Fourier transform spectrometers, regional aircraft, and the network of ground-based measurements. Here, we develop a method to infer simultaneous regional CO₂ and CH₄ flux estimates (Fig. 1) from the ratio of CH₄ and CO₂ dry-air mole fraction measurements (XCH₄ : XCO₂) retrieved from the Japanese Greenhouse gases Observing SATellite (GOSAT) using the proxy approach (based on University of Leicester proxy XCH₄ v4), which is less prone to systematic error from aerosols than the full physics approach (Schepers et al., 2012).

Two methods have been used to retrieve CO₂ and CH₄ columns from calibrated GOSAT L1B spectra: the “full physics” and “proxy” methods (Cogan et al., 2012; Parker et al., 2011). The full physics method uses an optimal estimation approach and incorporates a rigorous treatment of the atmospheric radiative transfer including the effects of clouds

and aerosols. This method uses optimized spectral windows to fit CO₂ and CH₄. The main advantage of this approach is the error characterization of the a posteriori state vector, and the main disadvantage is having to accurately characterize the atmospheric aerosol for the radiative transfer calculation. The proxy method, used to infer CH₄ columns, fits both gases in nearby spectral windows with the assumption that any fitting artefacts common to both gases (e.g. aerosol and clouds) will be removed by taking the ratio of the two gases. This method is simpler than the full physics approach and more robust against scattering, and as a result many more retrievals are possible from the GOSAT spectra. Interpretation of this ratio has in the past relied on scaling it with a model CO₂ column so that any erroneous model information about CO₂ can influence the interpretation of the GOSAT CH₄ columns (e.g. Parker et al., 2011; Fraser et al., 2013). We propose a method to simultaneously optimize CH₄ and CO₂ fluxes using the retrieved XCH₄ : XCO₂ ratio. This eliminates the need for a CO₂ model, removing the impact of model uncertainty on the retrieved methane columns, and increases the number of observations available to constrain CO₂ fluxes (Fig. 2).

In the following section we describe the space-borne and ground-based data used in our experiments. In Sect. 3 we describe the GEOS-Chem chemical transport model, and the maximum likelihood estimation (MLE) approach developed for this work. In Sect. 4 we report the GOSAT and model spatial and temporal distributions of XCH₄ : XCO₂ ratios (Sect. 4.1), test the MLE approach using a series of Observing System Simulation Experiments (OSSEs, Sect. 4.2) and present inversion results (Sect. 4.3). We conclude the paper in Sect. 5.

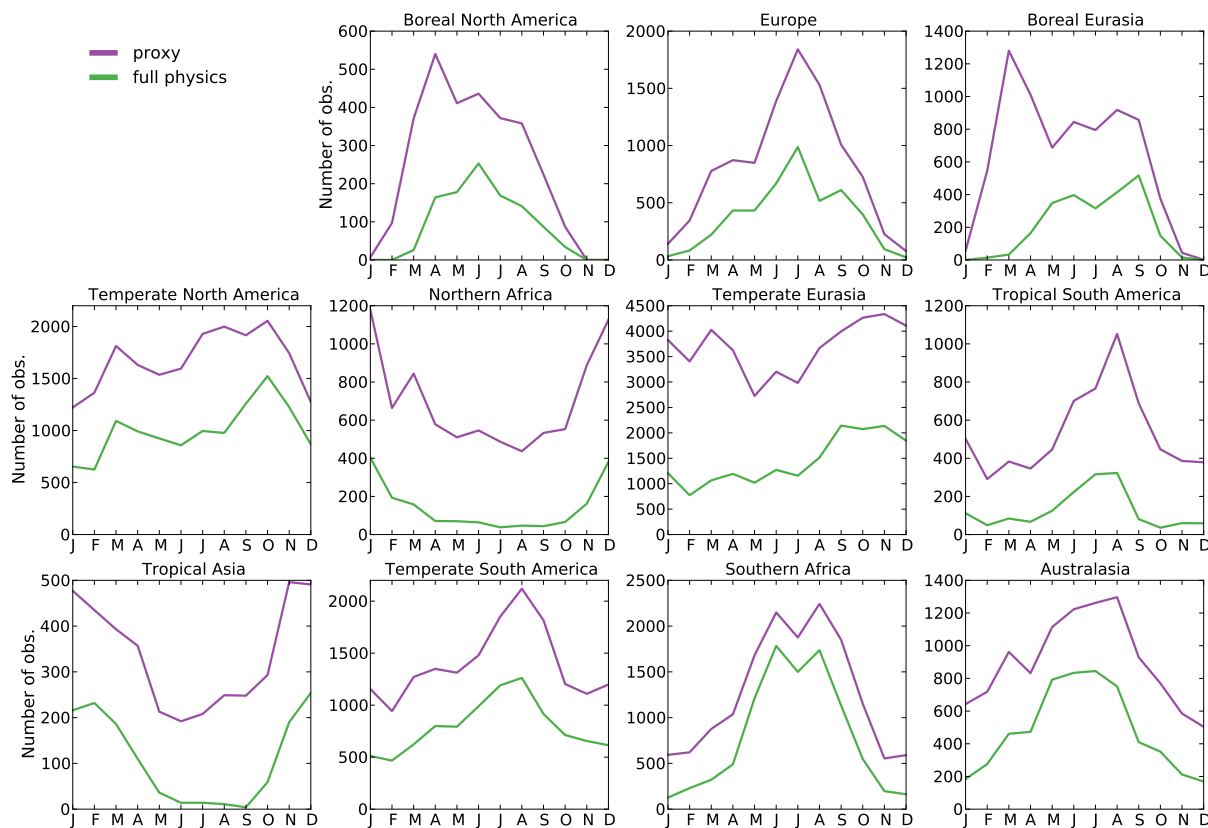


Figure 2. The number of GOSAT observations available per month during 2010 over specific geographical regions (Fig. 1) from the full-physics XCO₂ and proxy XCH₄ retrieval algorithms.

2 Data

2.1 GOSAT CO₂ and CH₄ atmospheric column-averaged mole fraction measurements

GOSAT was launched in 2009 by the Japanese Space Agency in a sun-synchronous orbit with an equatorial local overpass time of 13:00 LT, providing global coverage every three days (Kuze et al., 2009). GOSAT includes two instruments: TANSO-FTS (thermal and near infrared sensor for carbon observations – Fourier transform spectrometer) and TANSO-CAI (TANSO – cloud and aerosol imager). The TANSO-FTS instrument provides short-wave infrared (SWIR) radiances from which dry-air mole fraction observations of CO₂ and CH₄, XCO₂ and XCH₄ can be retrieved.

We provide a brief description of the proxy retrieval algorithm used for XCO₂ and XCH₄ and refer the reader to a detailed description (Parker et al., 2011). Here, we only consider nadir measurements. XCH₄ and XCO₂ that are retrieved at 1.65 μm and 1.61 μm, respectively. Past work has used this approach to infer observations of XCH₄ by scaling it by XCO₂, using XCO₂ as a proxy for the light path through the atmosphere. The mole fraction of XCH₄ is then obtained using a model estimate for XCO₂ so that XCH₄^{PROXY} =

$\left[\frac{\text{XCH}_4}{\text{XCO}_2}\right]^{\text{GOSAT}} \times \text{XCO}_2^{\text{MODEL}}$. However, using an inaccurate model of atmospheric CO₂ will introduce erroneous variability and bias in resulting values for XCH₄^{PROXY}. In this work we use the ratio $\left[\frac{\text{XCH}_4}{\text{XCO}_2}\right]^{\text{GOSAT}}$ directly, removing the requirement of model XCO₂.

We use cloud-screening and χ^2 quality-of-fit criteria, recommended by Parker et al. (2011), to filter retrieved XCH₄ : XCO₂ ratios. GOSAT surface pressure values, retrieved from the O₂ A-band for scenes with an estimated SNR > 50, are compared with colocated ECMWF surface pressure data. We discard cloudy scenes where the difference is > 30 hPa. We also discard data: (1) with solar zenith angles > 70° to remove data affected by long atmospheric path lengths and large incidence angles; (2) poleward of 60° latitude to minimize the model error due to the stratosphere; and (3) taken at medium gain (Fraser et al., 2013), as they can potentially include different biases than the high-gain data, and there are currently no sites to validate these medium-gain data. Here, we use version 4 of the proxy XCH₄ data, while our previous analysis Fraser et al. (2013) used version 3 of the data. Version 4 of the data includes an update to the GOSAT LIB data and its radiometric degradation, an update to the spectroscopic inputs and improvements to the a priori. Details about

Table 1. A priori sources of carbon dioxide and methane used in the GEOS-Chem model for 2010.

CO ₂	A priori magnitude (Gt year ⁻¹)	Reference
Fossil fuel	14.8	ODIAC (Oda and Maksyutov, 2011)
Oceans	-5.2	Takahashi et al. (2009)
Biosphere	3.4	CASA (Randerson et al., 1997)
Biomass burning	8.6	GFEDv3 (van der Werf et al., 2010)
CH ₄	A priori magnitude (Tg year ⁻¹)	Reference
Ruminant animals	92.8	EDGAR 3.2 FT (Olivier et al., 2005)
Coal mining	47.1	EDGAR 3.2 FT (Olivier et al., 2005)
Oil and natural gas production	42.8	EDGAR 3.2 FT (Olivier et al., 2005)
Landfills	44.7	EDGAR 3.2 FT (Olivier et al., 2005)
Rice	68.0	Bloom et al. (2012)
Wetlands	192.0	Bloom et al. (2012)
Biomass burning	19.4	GFEDv3 (van der Werf et al., 2010)
Oceans	15.1	Houweling et al. (1999)
Termites	20.1	Fung et al. (1991)
Hydrates	5.0	Fung et al. (1991)
Soil sink	-25.2	Fung et al. (1991)

the validation of this data product can be found in Sect. 6.2.3 of the ESA GHG-CCI Product Validation and Intercomparison Report (ESA GHG-CCI PVIR). The fractional differences between the final data products of v3 and v4, especially for XCH₄ : XCO₂, are small. For the full physics retrievals, due to the necessity of removing many more scenes affected by aerosol, the post-filtering requirements are much more stringent. This includes filters based on the retrieved aerosol amounts, geophysical characteristics of the scene (such as albedo and topography) and the consistency between Band 2 and Band 3 XCO₂. Figure 2 shows that the proxy method typically provides twice the number of observations available from the full physics approach.

2.2 In situ surface atmosphere mole fraction measurements

As described in Sect. 4.2, we use these in situ data as independent constraints for CH₄ and CO₂ emission estimates, improving the ability of the GOSAT proxy ratio to act as a constraint on both CH₄ and CO₂ flux estimates. We assimilate data from 45 sites of the NOAA Earth System Research Laboratory (ESRL), Global Monitoring Division, version 28 August 2013 (Dlugokencky et al., 2013); nine sites from the CSIRO Global Atmospheric Sampling Laboratory (GASLAB), released August 2013 (Francey et al., 1996); and two sites from Environment Canada's Greenhouse Gas Measurement Program (EC), released August 2013 (Worthy et al., 2003). Weekly air samples from all three networks are collected from sites distributed globally and data are reported on the NOAA 2004 (CH₄, all networks) and WMO X2007 (CO₂, ESRL, CSIRO) or WMO X83 (CO₂, EC) mole frac-

tion scales. Figure 1 shows the location of the sites used in this work. Three sites are in both the ESRL and GASLAB networks: Mauna Loa, Hawaii; Cape Grim, Tasmania; and the South Pole. Alert, Nunavut is in all three networks. At these sites we average the data from the available networks, leaving 51 individual sites.

3 Models

3.1 The GEOS-Chem transport model

We use version v9-01-03 of the GEOS-Chem global 3-D atmospheric chemistry transport model Bey et al. (2001), driven by assimilated meteorological fields from the NASA Global Modeling and Assimilation Office (version 5), to interpret observed variations of GOSAT proxy ratio measurements. We use the GEOS-5 meteorology at a horizontal resolution of 4° (latitude) × 5° (longitude) with 47 vertical levels that span from the surface to the mesosphere, with typically 35 levels in the troposphere.

The CH₄ and CO₂ simulations are described and evaluated against correlative data in Fraser et al. (2011) and Feng et al. (2011), respectively. Table 1 and Fig. 3 show the a priori global annual flux estimates and temporal distribution of CH₄ and CO₂ fluxes, respectively. The main atmospheric sink of CH₄ is the hydroxyl radical and is described in the troposphere by monthly mean 3-D fields generated by a full chemistry version of the model, which correspond to a methyl chloroform lifetime of 4.8±0.1 years. Loss rates for methane in the stratosphere are adapted from a 2-D stratospheric model (Wang et al., 2004).

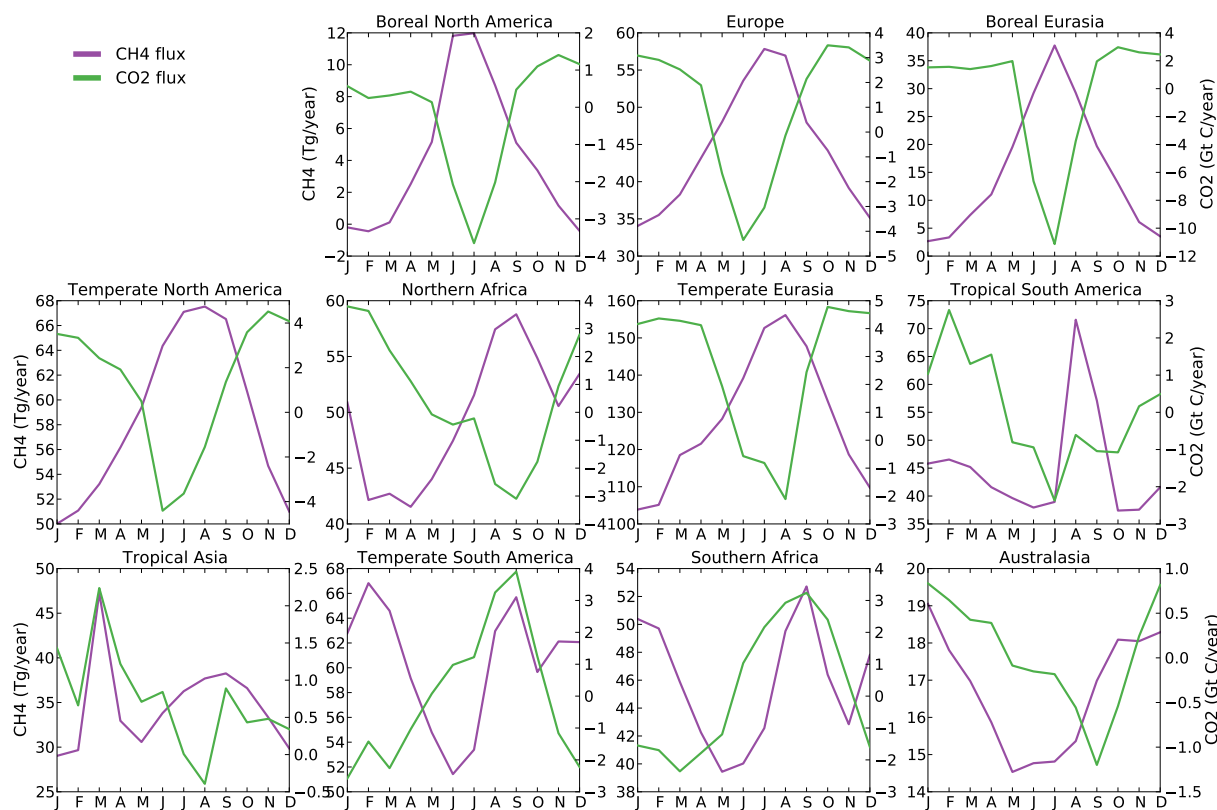


Figure 3. Monthly a priori emissions for CH₄ (Tg CH₄ year⁻¹) and CO₂ (Gt C year⁻¹) for the land regions shown in Fig. 1. Note the different y scales.

3.2 The MAP inverse model

We use an inverse model that finds the maximum a posteriori (MAP) solution (Rodgers, 2000) to simultaneously optimize the magnitude of the CH₄ and CO₂ flux estimates by fitting the a priori emission estimates, via the GEOS-Chem model (described above) to observations of GOSAT XCH₄ : XCO₂ ratios and in situ CH₄ and/or CO₂ mole fraction measurements. The MAP solution \hat{x} and the associated error covariance \hat{S} can be written as

$$\hat{x} = x_a + \left(\mathbf{K}^T \mathbf{S}_\epsilon^{-1} \mathbf{K} + \mathbf{S}_a^{-1} \right)^{-1} \mathbf{K}^T \mathbf{S}_\epsilon^{-1} (y - \mathbf{K}x_a) \quad (1)$$

$$\hat{S} = \left(\mathbf{K}^T \mathbf{S}_\epsilon^{-1} \mathbf{K} + \mathbf{S}_a^{-1} \right)^{-1}, \quad (2)$$

where x_a denotes the a priori vector, including a priori flux estimates of CO₂ and CH₄; y denotes the measurement vector, including the GOSAT XCH₄ : XCO₂ ratios and in situ CH₄ and/or CO₂ observations; \mathbf{K} denotes the Jacobian matrix, describing the sensitivity of model atmospheric concentrations to changes in the surface fluxes; \mathbf{S}_a denotes the a priori flux error covariance matrix; and \mathbf{S}_ϵ denotes the observation error covariance matrix. The superscripts T and ⁻¹ denote the matrix transpose and inverse operations, respectively.

For our implementation, x_a includes monthly CH₄ and CO₂ in 13 geographical regions (Fig. 1). We separate the fluxes into contributions from biomass burning, the biosphere, and anthropogenic activities. For CH₄, the biosphere includes contributions from wetlands, oceans, termites, hydrates, and the soil sink; and the anthropogenic activities include ruminant animals, coal mining, oil and natural gas production, landfills, and rice. For CO₂, the biosphere includes the land and ocean fluxes, and the anthropogenic activities include fossil fuel combustion. We optimize for the total flux from the global ice and ocean regions. The state vector has 840 elements made up of 11 continental regions including three sectors each for CO₂ and CH₄ for 12 months, and for ice and ocean regions for the two gases for the 12 months.

We construct \mathbf{S}_a as a diagonal matrix with the elements being the square of the error in the a priori fluxes, which we assume, guided by empirical studies, to be 100 % for the biospheric fluxes and 50 % for the biomass burning and anthropogenic fluxes. We assume no temporal correlation between fluxes in the same region or sector. We generally assume no correlation between CH₄ and CO₂ flux errors because they are not co-emitted, with the exception of biomass burning, for which we include a region-specific correlation with a mean value of 0.8 following previous empirical work Palmer et al. (2006). As we discuss below, this correlation

is a weak constraint for separating CH₄ and CO₂ from the observed XCH₄ : XCO₂ column ratios.

The measurement vector y includes a spatial and temporal average of GOSAT XCH₄ : XCO₂ ratio measurements. We average the data into monthly means for the 4° × 5° grid boxes of GEOS-Chem, which ensures a reasonable number of measurements for each month and increases the signal to noise of the observed ratio, as described below; we include the associated error in S_e . Estimates inferred using finer temporal and spatial bins tend to be noisier, largely reflecting changes in the measurement coverage from clouds and aerosols, but still produce consistent results shown here when they are averaged monthly and on the model grid. For some experiments, y also includes in situ surface measurements of CH₄ and/or CO₂.

We construct S_e as a diagonal matrix with the diagonal elements being the standard error of the mean measurement errors. For GOSAT, we use the a posteriori retrieval error from the v4 data product as described above. For surface data the measurement error is the standard error of the monthly mean calculated from the observations made over that month (Fraser et al., 2013). We also include a model transport error for each individual measurement error. For both the GOSAT ratio measurements and surface in situ data we describe this error as 0.25 % for (X)CO₂ (Feng et al., 2011) and 0.5 % for (X)CH₄ (Wang et al., 2004). When we average we sum these errors in quadrature.

The Jacobian matrix, K , is constructed from forward runs of the model where the fluxes in each region and for each sector are perturbed by 1 Gt for CO₂ or 1 Tg for CH₄. The model is then sampled at the time and location of the observations, smoothed using GOSAT averaging kernels, and these sensitivities are averaged into monthly and regional means.

4 Results

4.1 Forward modelling of GOSAT XCH₄ : XCO₂ ratios

Figure 3 shows that for many geographical regions CH₄ and CO₂ flux estimates are 6 months out of phase, reflecting seasonal changes in wetland emissions of CH₄ and terrestrial CO₂ fluxes. The opposing seasonal cycles will result in a partial cancellation of individual gas variations, and consequently may reduce the sensitivity of the ratio to variations in either gas.

Figure 4 shows the observed spatial variability of the annual mean XCH₄ : XCO₂ ratio is due mainly to XCH₄ variations. Common features to both the model and data include the interhemispheric gradient in the ratio and localized features due to orography, e.g. the Himalayan mountain range. The GEOS-Chem model reproduces the spatial pattern of the GOSAT ratio observations within $\simeq 2.5\%$. The model has a negative bias over the tropics (1–2%), which is largely due to the model positive bias for XCO₂ that reflects errors in

the a priori natural flux inventories. This figure illustrates the demanding accuracy and precision requirements associated with this space-borne measurement if it is to become a useful constraint for carbon cycle science. The monthly variation of observed values, here shown as the 1- σ value expressed as a percentage about the annual mean, is smaller for the XCH₄ : XCO₂ ratios for which scattering and other biases are removed than XCH₄ or XCO₂.

Figure 5 shows that the model can typically capture 70 % of the observed temporal variability of XCH₄ : XCO₂ over different geographical regions. Over most regions we find the model has a small but growing negative bias, reflecting its overestimation of the CO₂ growth rate. The model generally agrees best with GOSAT in the Northern Hemisphere extratropics, and worst over Tropical South America, where we know the model underestimates the CO₂ biological uptake. While XCH₄ variations determine the spatial distribution of the GOSAT XCH₄ : XCO₂ ratio, we find that XCO₂ determines its seasonal cycle. This is particularly noticeable over Boreal regions and Europe, where the peak in the ratio in the second half of the year is a result of decreasing XCO₂ due to increased uptake from the biosphere.

Figure 5 also illustrates the importance of using the ratio instead of the contributory columns. Both XCH₄ and XCO₂ are too noisy (due to variations in the atmosphere and surface) by themselves but common retrieval errors will cancel out in the ratio. Please note that the XCH₄ and XCO₂ plotted here are not the final data products from GOSAT, but the intermediary products from which the ratio is calculated. Comparing this figure to Fig. 5 in Cogan et al. (2012) and Fig. 3 in Parker et al. (2011) shows that the regional bias between GOSAT and the model is much smaller in the ratio than in the individual species. While GEOS-Chem tends to underestimate the GOSAT ratio, the bias is more or less consistent between regions, which is not the case for either XCO₂ or XCH₄.

4.2 Inverse modelling of GOSAT XCH₄ : XCO₂ ratios: OSSEs

We use OSSEs, realistic numerical experiments, to characterize the method we use to estimate simultaneously CO₂ and CH₄ regional fluxes from GOSAT XCH₄ : XCO₂ ratios. For all these experiments, we sample the model at the location of the clear-sky GOSAT observations, apply GOSAT averaging kernels, and add, as a minimum, random error based on actual GOSAT measurements. Similarly, we sample the model at the time and location of the surface observations and add characteristic random noise informed by the data.

We conduct four broad sets of OSSEs: (1) those that use only the GOSAT XCH₄ : XCO₂ ratios, (2) those that use the GOSAT data and in situ measurements of CH₄ and/or CO₂, (3) those that use the best setup from (2) and vary the a priori fluxes, and (4) as (3) but including regional bias.

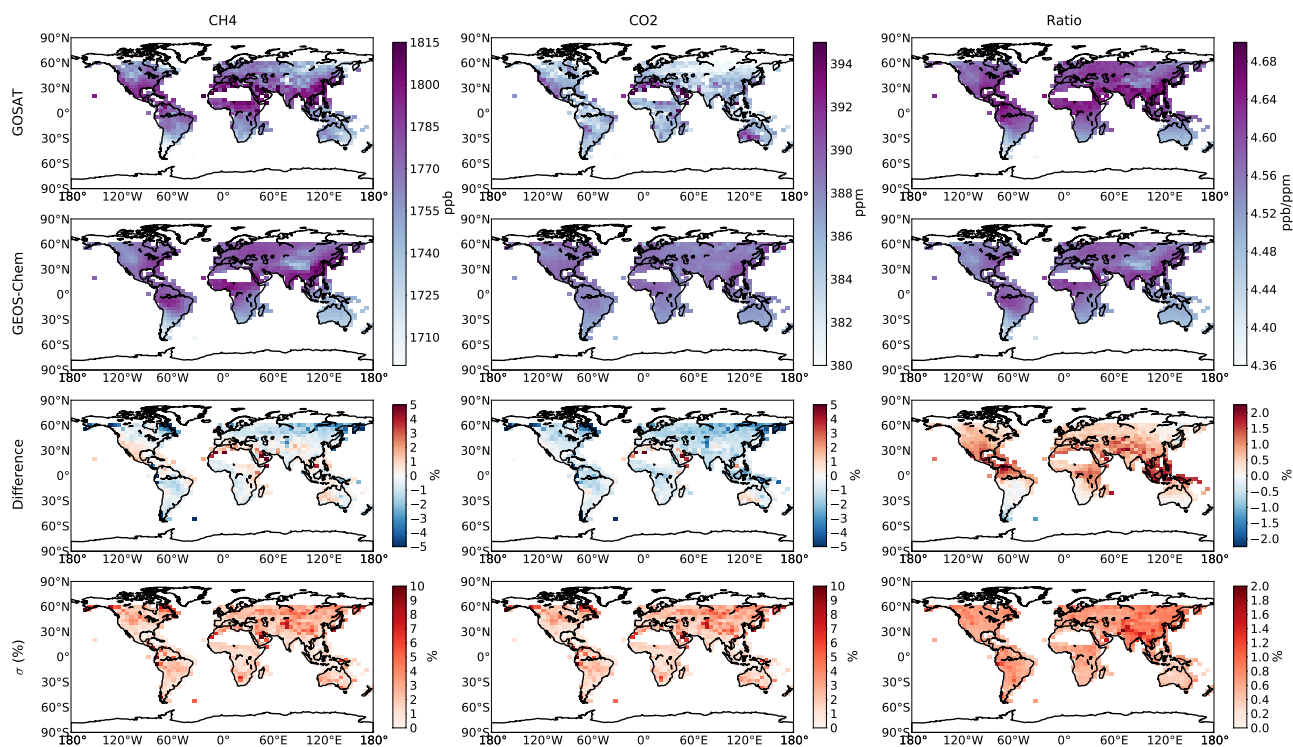


Figure 4. Annual mean GOSAT (top row) and GEOS-Chem model (second row) XCH₄, XCO₂, and XCH₄ : XCO₂ ratio measurements from GOSAT during 2010 averaged on the model 4° × 5° grid. The third row shows the percentage difference between them (GOSAT minus GEOS-Chem). For XCH₄ and XCO₂, we truncate at the mean ± 2-σ. The bottom row shows the 1-σ value in the difference as a percentage about the annual mean GOSAT XCH₄, XCO₂, and XCH₄ : XCO₂ data. The model has been sampled at the time and location of the GOSAT observations, and convolved with scene-dependent averaging kernels.

Figure 6a and b show the results from experimental set (1). First, we assume that the a priori fluxes equal the true fluxes, allowing us to assess the level of numerical noise in the closed-loop system. We find that after setting the a priori to the true fluxes there is only a small mean difference between a posteriori and true fluxes that is within the uncertainty of the a posteriori fluxes. We then assume that the a priori fluxes are scaled by 20 % relative to the truth, allowing us to assess the efficacy with which the synthetic observations can recover the true flux estimates. Because CO₂ and CH₄ fluxes have different geographical distributions, the simultaneous increase will not necessarily cancel out in the ratio. For this scaling experiment the observing system reconciles the model minus observation difference by simultaneously changing the CH₄ and CO₂ fluxes that are not always within the a posteriori flux uncertainties, which we attribute to the fact that there is no additional information about allocating this difference to a particular gas.

Figure 6c–e show results from experimental set (2). Adding either CH₄ or CO₂ surface observations to the measurement vector reduces the bias between the a posteriori and true fluxes (by up to nearly 100 %), but also reduces the error reduction of the other species. We find that assimilating both CH₄ and CO₂ surface observations gives the smallest differ-

ence from the truth and the largest error reductions; we adopt this as our control experimental setup in the following sections. We accept the larger standard deviations as the fluxes are closer to the truth. For reference, using only the surface data returns error reductions of approximately 23 % for both species (not shown). Figure 7 shows the results from experimental set (3). This control observing system can return the true fluxes for a wide array of varying CH₄ and CO₂ fluxes for most geographical regions.

In experiment set (4) (not shown) we assess the impact of a prescribed observation bias to the GOSAT data on the a posteriori flux estimates; assuming that the surface data is unbiased or at least can be identified readily via ongoing calibration/validation activities. We assume a latitudinally varying bias that is superimposed onto the “true” atmospheric measurements plus random error (0.005 ppb ppm⁻¹) for the monthly gridded measurement vector. To describe the latitudinal bias, we use a second-order polynomial with a minimum at the South Pole and a maximum at the North Pole; our choice of this polynomial is based on the bias between the model and GOSAT data. This bias ranges from −0.08 to 0.06 ± 0.005 ppb ppm⁻¹. We conduct two parallel experiments: (i) we assume the data was unbiased and (ii) we assume and fit a fourth-degree polynomial as a function of lat-

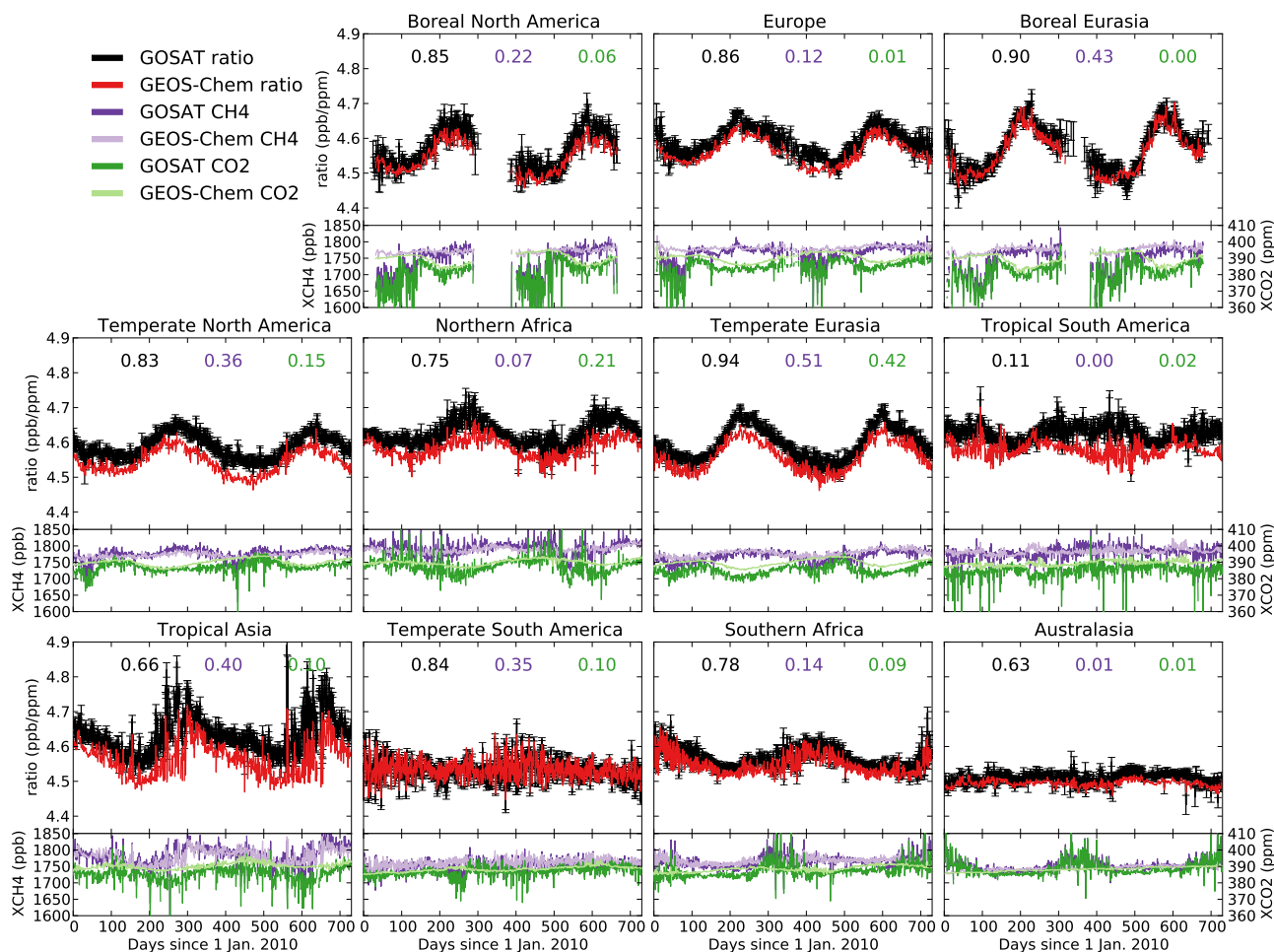


Figure 5. GOSAT and GEOS-Chem daily mean XCH₄ : XCO₂ ratios (top panels) for 2010–2011, averaged over each land region shown in Fig. 1. Squared Pearson correlation coefficients between GOSAT and GEOS-Chem are shown inset for the ratio (black), XCH₄ (purple), and XCO₂ (green). Bottom panels show the corresponding GOSAT and GEOS-Chem daily mean XCH₄ and XCO₂. The model has been sampled at the time and location of the GOSAT observations, and convolved with scene-dependent averaging kernels.

itude to the mean annual difference between the model and data. We find that using higher degree polynomials did not significantly change our results. For experiment (4i), the resulting CH₄ and CO₂ fluxes are up to 10 Tg and 0.4 Gt different from the true fluxes, respectively. For experiment (4ii), we find that the bias correction returns values that are closer to the true fluxes.

4.3 Analysis of GOSAT XCH₄ : XCO₂ ratios

Figure 8 and Table 2 show flux estimates inferred from GOSAT XCH₄ : XCO₂ data and surface mole fraction observations of CH₄ and CO₂ (Sect. 2), and independent flux estimates of CH₄ and CO₂ inferred using an ensemble Kalman filter (EnKF) from GOSAT XCH₄ proxy data (Fraser et al., 2013) and XCO₂ full physics data together with the corresponding surface stations (Feng et al., 2011; Chevallier et al., 2014).

For CH₄, the general tendency of a posteriori fluxes, relative to a priori values, is consistent between the XCH₄ : XCO₂ ratio and the proxy XCH₄ data, but based on a posteriori uncertainties the magnitude of these fluxes can be statistically different. The ratio infers larger emissions from Tropical South America, Northern Africa, and Temperate Eurasia. Error reductions resulting from assimilating XCH₄ : XCO₂ ratio data are typically 30 % but can be up to 60 % (Temperate Eurasia). For some regions, the error reduction from using the ratio is larger than from using the individual gas but for others the reduction is smaller. Geographical regions with notable improvements in our understanding from assimilating the ratio data include Tropical and Temperate South America, Northern Africa, and Temperate Eurasia. These regions all have observed seasonal cycles in the ratio that are larger than a few percent of the annual mean, allowing the ratio data to better inform the a priori. Strictly speaking we cannot directly compare the CH₄ flux estimated reported

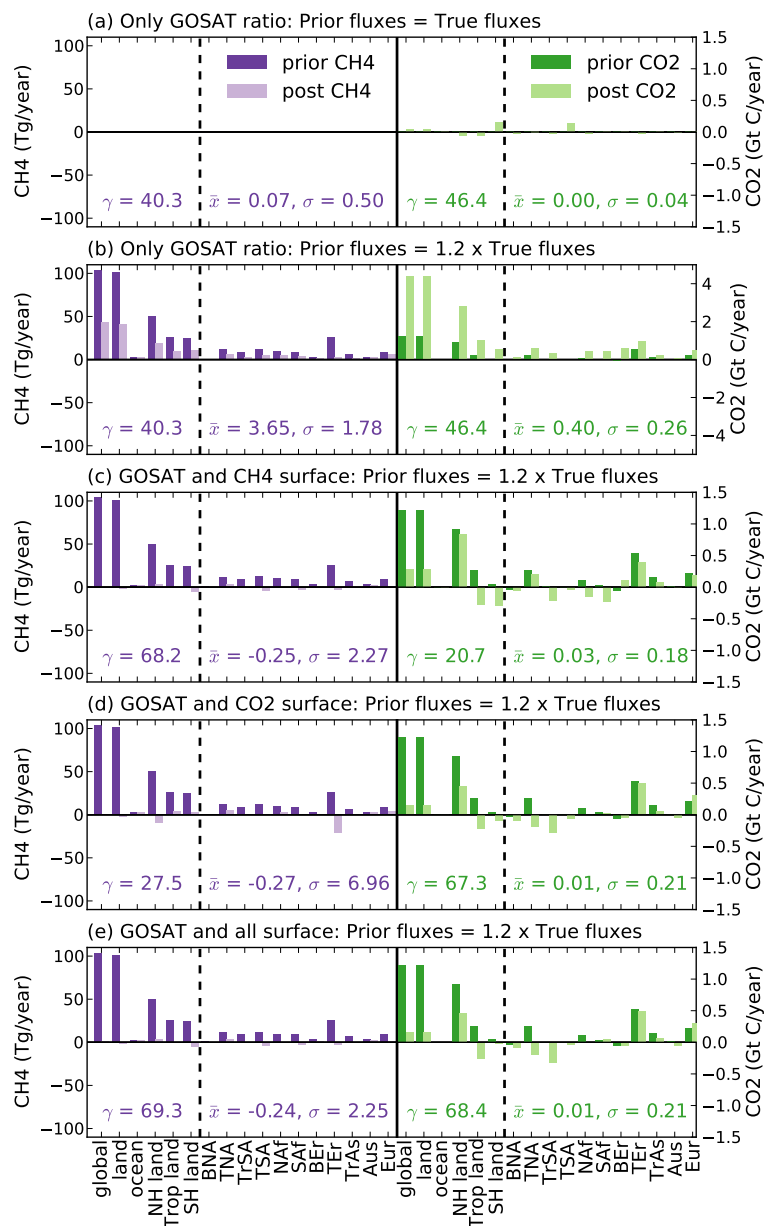


Figure 6. Annual regional flux estimates of CH₄ (left) and CO₂ (right) inferred from various observing system simulation experiments, where values are described as the departure from the corresponding true flux. The first six regions are aggregates: global represents all regional fluxes; land omits the oceans and vice versa; NH land sums fluxes from Boreal and Temperate North America, Europe, and Boreal and Temperate Eurasia; Trop land sums fluxes from Tropical South America, Northern Africa, and Tropical Asia; and SH land sums fluxes from Temperate South America, Southern Africa, and Australasia. The remaining regions are defined in Fig. 1. For experiment (a) the a priori and the truth are the same and only GOSAT data are used; experiment (b) is as (a) but the a priori fluxes are 20 % higher than the truth; experiment (c) is as (b) but CH₄ surface flask data are also used; experiment (d) is as (b) but CO₂ surface flask data are also used; experiment (e) is as (b) but CH₄ and CO₂ surface flask data are also used. Note the different y-scale for CO₂ in (b). The error reduction in the global fluxes (γ), the mean (\bar{x}) and standard deviation (σ) of the difference in the individual regions are shown inset in each panel.

by Fraser et al. (2013) and those inferred from the XCH₄ : XCO₂ ratio data. As noted above we are using a newer version of the proxy retrieval that includes updated a priori information particularly for stratospheric CH₄ concentrations and updates to the retrieval grid and spectroscopic input, re-

sulting in 5–10 % more clear-sky measurements; we are using a newer version of the GEOS-Chem transport model; and most importantly we treat the measurements differently, reflecting the difficulty in the small observed changes in the XCH₄ : XCO₂ ratio data.

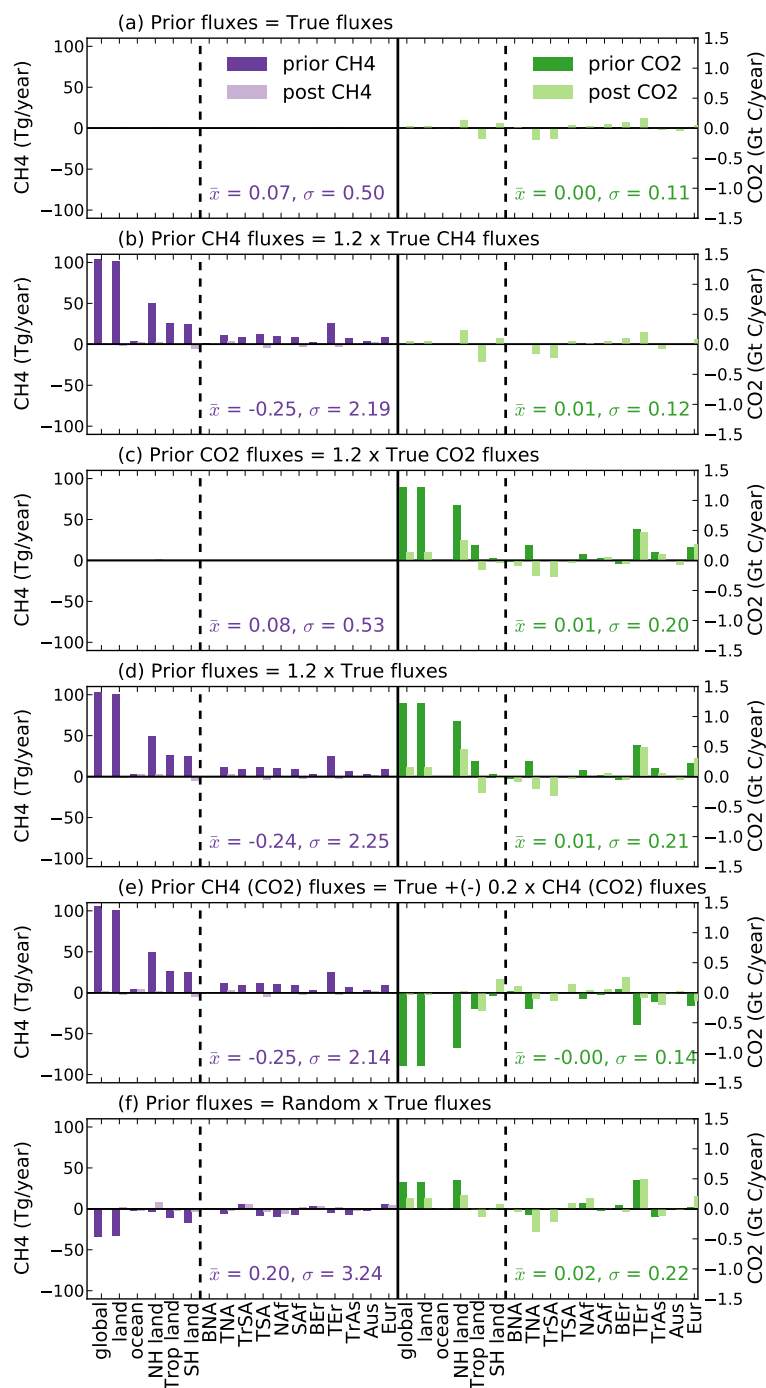


Figure 7. As Fig. 6 but all experiments use CH₄ and CO₂ surface flask data and GOSAT data. For experiment (a) a priori fluxes are equal to the true fluxes; for experiment (b) CH₄ a priori fluxes are 20% larger than the true fluxes; for experiment (c) CO₂ a priori fluxes are 20% larger than the true fluxes; for experiment (d) CH₄ and CO₂ a priori fluxes are 20% larger than their true fluxes; for experiment (e) CH₄ a priori fluxes are 20% larger and CO₂ a priori fluxes are 20% smaller than their true fluxes; and for experiment (f) all a priori fluxes are perturbed stochastically, ranging from -20 to 20% , from the true fluxes.

For CO₂, a posteriori fluxes inferred from the GOSAT ratio can be statistically different to those inferred from the EnKF inversion, including Tropical South America, Southern Africa, Boreal Eurasia, Tropical Asia, and Australasia.

These differences between the inversion largely reflect the larger volume of XCH₄ : XCO₂ ratio data resulting in better spatial and temporal coverage (Fig. 2). We may also expect the largest differences for regions where we believe there are

Table 2. A priori and a posteriori CH₄ and CO₂ regional land fluxes (natural+anthropogenic) and 1- σ uncertainties inferred from GOSAT XCH₄ : XCO₂ and in situ mole fraction measurements. Fluxes inferred from previous work – Fraser et al. (2013); Feng et al. (2011) – using an EnKF are denoted EnKF. CH₄ and CO₂ fluxes are reported as Tg CH₄ year⁻¹ and Gt C year⁻¹, respectively.

Region	CH ₄ prior		CH ₄ posterior (this work)		CH ₄ posterior (EnKF)		CO ₂ prior		CO ₂ posterior (this work)		CO ₂ posterior (EnKF)	
	Flux	1- σ	Flux	1- σ	Flux	1- σ	Flux	1- σ	Flux	1- σ	Flux	1- σ
Boreal North America	4.1	1.0	4.0	0.9	4.8	0.9	-0.4	0.5	-0.7	0.3	0.1	0.1
Europe	44.5	3.6	31.3	2.4	39.8	2.3	0.5	0.8	0.6	0.4	0.6	0.2
Boreal Eurasia	15.2	2.5	19.3	1.9	15.0	2.5	-0.7	1.0	-1.5	0.9	-0.4	0.2
Temperate North America	58.5	4.1	62.5	3.6	64.9	3.1	0.9	0.8	1.2	0.5	1.4	0.2
Northern Africa	49.6	4.3	65.6	3.5	46.8	4.2	0.3	0.6	0.4	0.5	0.2	0.2
Temperate Eurasia	127.9	11.8	140.2	4.4	124.0	6.5	2.7	0.7	3.4	0.4	3.4	0.2
Tropical South America	45.1	5.6	59.0	3.1	51.1	4.1	-0.2	0.5	0.3	0.3	-0.3	0.3
Tropical Asia	34.6	4.5	40.6	3.2	42.9	3.1	0.7	0.2	0.9	0.2	1.5	0.2
Temperate South America	60.5	5.8	50.9	3.3	55.8	5.6	-0.4	0.6	-0.6	0.4	-0.5	0.3
Southern Africa	46.0	5.1	43.6	3.6	41.4	3.1	-1.4	0.8	-1.9	0.6	0.1	0.2
Australasia	16.7	1.4	17.9	1.3	17.8	1.3	-0.1	0.2	-0.4	0.2	0.7	0.2

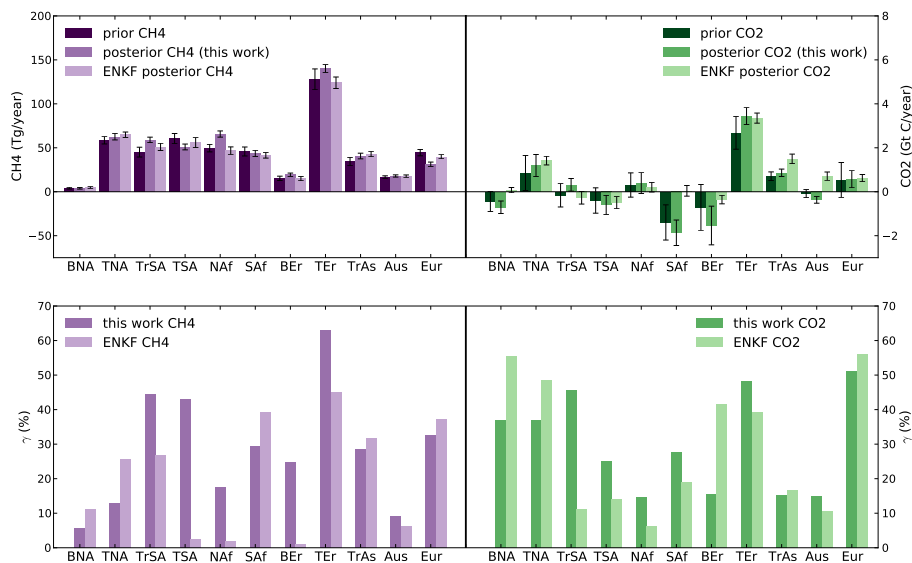


Figure 8. A priori and a posteriori CO₂ and CH₄ regional land fluxes (natural + anthropogenic) inferred from GOSAT XCH₄ : XCO₂ and surface measurements of CO₂ and CH₄ and from XCO₂ or XCH₄ using an EnKF (top) (Feng et al., 2011; Fraser et al., 2013), and the corresponding reduction in uncertainty (bottom), during 2010. Error bars atop emission estimates represent the 1- σ uncertainty.

the greatest biases in the proxy XCH₄ and full physics XCO₂ retrievals. We find that the associated error reductions for the CO₂ fluxes inferred from the XCH₄ : XCO₂ ratio data are generally larger than those for CH₄, and are different from those inferred from the EnKF inversion.

5 Concluding remarks

We have interpreted measurements of XCH₄ : XCO₂ from GOSAT in which XCH₄ and XCO₂ are retrieved in nearby spectral windows under the assumption that their ratio will largely remove common sources of biases. By interpreting

the ratio directly we minimize any bias introduced by model XCO₂; although we acknowledge that other sources of model bias remain. A major advantage of the ratio is this data product does not suffer from the measurement bias that can befall the full physics XCO₂ and CH₄ data. Another advantage is that the volume of these data is greater than their full physics counterpart. While the ratio benefits from these three advantages, the differences between model and observed quantities are much smaller (typically < $\pm 2\%$) than the corresponding changes in XCO₂ or XCH₄ and consequently comparable in magnitude to other sources of error, e.g. model transport error, that cannot easily be characterized and removed. By us-

ing the ratio we may be reaching the limitations on the precision of these data and our ability to interpret them using current transport models. However, over particular geographical regions we find there are seasonally varying GOSAT minus model ratio differences that are large enough to be exploited, e.g. Tropical South America and Tropical Asia.

Using a series of numerical experiments we showed that the simultaneous estimation of CO₂ and CH₄ fluxes using the GOSAT ratio is possible with the information split as a function of the a priori uncertainties; however, the inversion system returns unphysical fluxes in some regions. We showed that including surface mole fraction measurements of CO₂ and CH₄ in the measurement vector provides an “anchor” for the inversion, and that the combined GOSAT and surface data can distinguish between CO₂ and CH₄ flux adjustments.

Using real data for 2010 we showed that the combination of the GOSAT XCH₄ : XCO₂ ratio and the surface mole fraction data led to comparable flux estimates inferred from the proxy XCH₄ and full physics XCO₂ data, but outcompeted these individual data products over geographical regions where there was a seasonal cycle larger than a few percent of the annual mean. For instance, over Tropical South America we found a small but significant emission of CO₂ while analysis of the full physics XCO₂ showed a small sink term. Analysis of the ratio led to slightly larger reductions globally, and in some regions, primarily in the tropics, much larger reductions in uncertainty of CO₂ and CH₄. Given that the ratio data are less compromised by systematic biases than the proxy XCH₄ and full physics XCO₂ data products, we more generally argue that that the corresponding a posteriori flux estimates and their uncertainties provide a more faithful description of regional fluxes.

The main reasons for using the XCH₄ : XCO₂ ratio are that it minimizes scattering and potentially other biases and significantly increases geographical coverage. Although CO₂ and CH₄ do not share many common sources that result in significant atmospheric covariance, we have shown the following: (1) the combined information from these two gases can be disentangled using other data, and (2) flux estimates inferred from the XCH₄ : XCO₂ ratio are an improvement over what can be achieved using observations of either full-physics XCO₂ or XCH₄. Consequently, the use of spaceborne observations of the XCH₄ : XCO₂ ratio will be of particular interest for estimating CO₂ surface fluxes over regions that are characterized by frequent cloud cover and high aerosol loading such as the tropics, where the quality and coverage of full-physics XCO₂ retrieval approaches will be limited even for missions with spatial footprints smaller than GOSAT. This ratio approach could also be used in combination with other atmospheric tracers that help improve the source attribution of CO₂, e.g. carbon monoxide, where the ensuing correlation is driven by incomplete combustion (Palmer et al., 2006). Space-borne mission concept development related to the carbon cycle should focus not only on the primary compound but also on any secondary compound

that will help interpret the observed variability of that primary gas.

Acknowledgements. We thank Doug Worthy for the Environment Canada data. NOAA ESRL is supported by NOAA's Climate Program Office; and CSIRO research at Cape Grim is supported by the Australian Bureau of Meteorology. A. Fraser and R. Parker were supported by the Natural Environment Research Council National Centre for Earth Observation (NCEO). L. Feng was partly funded by the “Data Assimilation Project – Interfacing EO data with atmospheric and land surface models” ESA contract 4000104980/1-LG. H. Bösch, R. Parker and L. Feng also acknowledge funding by the ESA Climate Change Initiative (GHG-CCI). P. I. Palmer gratefully acknowledges his Royal Society Wolfson Research Merit Award.

Edited by: B. N. Duncan

References

- Bey, I., Jacob, D. J., Yantosca, R. M., Logan, J. A., Field, B., Fiore, A. M., Li, Q., Liu, H., Mickley, L. J., and Schultz, M.: Global modeling of tropospheric chemistry with assimilated meteorology: Model description and evaluation, *J. Geophys. Res.*, 106, 23073–23096, 2001a.
- Bloom, A. A., Palmer, P. I., Fraser, A., and Reay, D. S.: Seasonal variability of tropical wetland CH₄ emissions: the role of the methanogen-available carbon pool, *Biogeosciences*, 9, 2821–2830, doi:10.5194/bg-9-2821-2012, 2012.
- Chevallier, F., Palmer, P. I., Feng, L., Boesch, H., O'Dell, C., W., and Bousquet, P.: Toward robust and consistent regional CO₂ flux estimates from in situ and spaceborne measurements of atmospheric CO₂, *Geophys. Res. Lett.*, 41, 1065–1070, doi:10.1002/2013GL058772, 2014.
- Cogan, A. J., Boesch, H., Parker, R. J., Feng, L., Palmer, P. I., Blavier, J.-F. L., Deutscher, N. M., Macatangay, R., Notholt, J., Roehl, C., Warneke, T., and Wunch, D.: Atmospheric carbon dioxide retrieved from the Greenhouse gases Observing SATellite (GOSAT): comparison with ground-based TCCON observations and GEOS-Chem model calculations, *J. Geophys. Res.*, 117, D21301, doi:10.1029/2012JD018087, 2012.
- Dlugokencky, E. J., Lang, P. M., Crotwell, A., Masarie, K. A., and Crotwell, M.: Atmospheric methane dry air mole fractions from the NOAA ESRL carbon cycle cooperative global air sampling network, 1983–2012, Version: 2013-08-28, available at: ftp://afpt.cmdl.noaa.gov/data/trace_gases/ch4/flask/surface/ (last access: September 2013), 2013.
- Feng, L., Palmer, P. I., Yang, Y., Yantosca, R. M., Kawa, S. R., Paris, J.-D., Matsueda, H., and Machida, T.: Evaluating a 3-D transport model of atmospheric CO₂ using ground-based, aircraft, and space-borne data, *Atmos. Chem. Phys.*, 11, 2789–2803, doi:10.5194/acp-11-2789-2011, 2011.
- Francey, R. J., Steele, L. P., Langenfelds, R. L., Lucarelli, M. P., Allison, C. E., Beardsmore, D. J., Coram, S. A., Derek, N., de Silva, F. R., Etheridge, D. M., Fraser, P. J., Henry, R. J., Turner, B., Welch, E. D., Spencer, D. A., and Cooper, L. N.:

- Global Atmospheric Sampling Laboratory (GASLAB): supporting and extending the Cape Grim trace gas programs, in: Baseline Atmospheric Program (Australia), Bureau of Meteorology and CSIRO Division of Atmospheric Research, Melbourne, Australia, 8–29, 1996.
- Fraser, A., Chan Miller, C., Palmer, P. I., Deutscher, N. M., Jones, N. B., and Griffith, D. W. T.: The Australian methane budget: interpreting surface and train-borne measurements using a chemistry transport model, *J. Geophys. Res.*, 116, D20306, doi:10.1029/2011JD015964, 2011.
- Fraser, A., Palmer, P. I., Feng, L., Boesch, H., Cogan, A., Parker, R., Dlugokencky, E. J., Fraser, P. J., Krummel, P. B., Langenfelds, R. L., O'Doherty, S., Prinn, R. G., Steele, L. P., van der Schoot, M., and Weiss, R. F.: Estimating regional methane surface fluxes: the relative importance of surface and GOSAT mole fraction measurements, *Atmos. Chem. Phys.*, 13, 5697–5713, doi:10.5194/acp-13-5697-2013, 2013.
- Fung, I., John, J., Lerner, J., Matthews, E., Prather, M., Steele, L. P., and Fraser, P. J.: Three-dimensional model synthesis of the global methane cycle, *J. Geophys. Res.*, 96, 13033–13065, doi:10.1029/91JD01247, 1991.
- Gurney, K. R., Law, R. M., Denning, A. S., Rayner, P. J., Baker, D., Bousquet, P., Bruhwiler, L., Chen, Y.-H., Ciais, P., Fan, S., Fung, I. Y., Gloor, M., Heimann, M., Higuchi, K., John, J., Maki, T., Maksyutov, S., Masarie, K., Peylin, P., Prather, M., Pak, B. C., Randerson, J., Sarmiento, J., Taguchi, S., Takahashi, T., and Yuen, C.-W.: Towards robust regional estimates of CO₂ sources and sinks using atmospheric transport models, *Nature*, 415, 626–630, doi:10.1038/415626a, 2002.
- Houweling, S., Kaminski, T., Dentener, F., Lelieveld, J., and Heimann, M.: Inverse modeling of methane sources and sinks using the adjoint of a global transport model, *J. Geophys. Res.*, 104, 26137–26160, doi:10.1029/1999JD900428, 1999.
- Kuze, A., Suto, H., Nakajima, M., and Hamazaki, T.: Thermal and near infrared sensor for carbon observation Fourier-transform spectrometer on the Greenhouse Gases Observing Satellite for greenhouse gases monitoring, *Appl. Optics*, 48, 6716–6733, doi:10.1364/AO.48.006716, 2009.
- Oda, T. and Maksyutov, S.: A very high-resolution (1 km × 1 km) global fossil fuel CO₂ emission inventory derived using a point source database and satellite observations of nighttime lights, *Atmos. Chem. Phys.*, 11, 543–556, doi:10.5194/acp-11-543-2011, 2011.
- Olivier, J. G. J., van Aardenne, J. A., Dentener, F., Ganzeveld, L., and Peters, J. A. H. W.: Recent trends in global greenhouse gas emissions: regional trends and spatial distribution of key sources, in: Non-CO₂ Greenhouse Gases (NCGG-4), edited by: van Amstel, A., Millpress, Rotterdam, 325–330, 2005.
- Palmer, P., Suntharalingam, P., Jones, D., Jacob, D., Streets, D., Fu, Q., Vay, S., and Sachse, G.: Using CO₂ : CO correlations to improve inverse analyses of carbon fluxes, *J. Geophys. Res.*, 111, D12318, doi:10.1029/2005JD006697, 2006.
- Parker, R., Boesch, H., Cogan, A., Fraser, A., Feng, L., Palmer, P. I., Messerschmidt, J., Deutscher, N., Griffith, D. W., Notholt, J., Wennberg, P. O., and Wunch, D.: Methane observations from the Greenhouse Gases Observing SATellite: comparison to ground-based TCCON data and model calculations, *Geophys. Res. Lett.*, 38, L15807, doi:10.1029/2011GL047871, 2011.
- Randerson, J., Thompson, M., Conway, T., Fung, I., and Field, C.: The contribution of terrestrial sources and sinks to trends in the seasonal cycle of atmospheric carbon dioxide, *Global Biogeochem. Cy.*, 11, 535–560, 1997.
- Rodgers, C. D.: *Inverse Methods for Atmospheric Sounding: Theory and Practice*, World Scientific Publishing, River Edge, NJ, 2000.
- Schepers, D., Guerlet, S., Butz, A., Landgraf, J., Frankenberg, C., Hasekamp, O., Blavier, J.-F., Deutscher, N. M., Griffith, D. W. T., Hase, F., Kyro, E., Morino, I., Sherlock, V., Sussmann, R., and Aben, I.: Methane retrievals from Greenhouse Gases Observing Satellite (GOSAT) shortwave infrared measurements: performance comparison of proxy and physics retrieval algorithms, *J. Geophys. Res.*, 117, D10307, doi:10.1029/2012JD017549, 2012.
- Takahashi, T., Sutherland, S. C., Wanninkhof, R., Sweeney, C., Feely, R. A., Chipman, D. W., Hales, B., Friederich, G., Chavez, F., Sabine, C., Watson, A., Bakker, D. C., Schuster, U., Metzl, N., Yoshikawa-Inoue, H., Ishii, M., Midorikawa, T., Nojiri, Y., Körtzinger, A., Steinhoff, T., Hoppema, M., Olafsson, J., Arnarson, T. S., Tilbrook, B., Johannessen, T., Olsen, A., Bellerby, R., Wong, C., Delille, B., Bates, N., and de Baar, H. J.: Climatological mean and decadal change in surface ocean pCO₂, and net sea-air {CO₂} flux over the global oceans, *Deep-Sea Res. Pt. II*, 56, 554–577, doi:10.1016/j.dsr2.2008.12.009, 2009.
- van der Werf, G. R., Randerson, J. T., Giglio, L., Collatz, G. J., Mu, M., Kasibhatla, P. S., Morton, D. C., DeFries, R. S., Jin, Y., and van Leeuwen, T. T.: Global fire emissions and the contribution of deforestation, savanna, forest, agricultural, and peat fires (1997–2009), *Atmos. Chem. Phys.*, 10, 11707–11735, doi:10.5194/acp-10-11707-2010, 2010.
- Wang, J. S., Logan, J. A., McElroy, M. B., Duncan, B. N., Megretskaia, I. A., and Yantosca, R. M.: A 3-D model analysis of the slowdown and interannual variability in the methane growth rate from 1988 to 1997, *Global Biogeochem. Cy.*, 18, GB3011, doi:10.1029/2003GB002180, 2004.
- Worthy, D. E., Platt, J. A., Kessler, R., Ernst, M., and Racki, S.: The Greenhouse Gases Measurement Program, measurement procedures and data quality, in: Canadian Baseline Program; Summary of Progress to 2002, Meteorological Service of Canada, Quebec, 97–120, 2003.